RSC Advances

ROYAL SOCIETY OF CHEMISTRY

www.rsc.org/advances

RSC Advances

$SnCl_4$-Functionalized nano-Fe_3O_4 encapsulated-silica particles as a novel heterogeneous solid acid for synthesis of 1,4-dihydropyridine derivatives

Received 00th January 20xx,
Accepted 00th January 20xx

DOI: 10.1039/x0xx00000x

www.rsc.org/

Abdolhamid Bamoniri*, Sara Fouladgar

A novel type of green heterogeneous solid acid was prepared by the immobilization of $SnCl_4$ on the surface of Fe_3O_4@SiO_2 (Fe_3O_4@SiO_2-$SnCl_4$) and characterized by Fourier transform-infrared spectroscopy (FT-IR), X-ray diffraction (XRD), vibrating sample magnetometer (VSM), field emission-scanning electron microscope (FE-SEM), energy dispersive X-ray (EDX), N_2 adsorption-desorption (BET) and transmission electron microscope (TEM). The activity of this solid acid was probed *via* the synthesis of 1,4-dihydropyridine derivatives of three or four components coupling reaction of aldehyde, 1,3-dicabonyl compound, and ammonium acetate under ultrasonic irradiation and yeilded excellent results with easy work-up in short time. 1,4-dihydropyridine derivatives were characterized by FT-IR and ^{1}HNMR

.

Introduction

Industrial chemistry is broadly adopting the conception of green chemistry to meet the essential scientific challenges of protecting the environment and human health while preserving commercial viability.[1] As one of the breakthroughs progresses in the field of green processes based on sonochemistry, it has increasingly been considered as a simple, clean and convenient method[2-5] and so chemists are focusing on its use for the synthesis of organic compounds Similarly, multicomponent reactions (MCRs) work as an efficient and important tool in modern synthetic organic chemistry. These reactions which consist of two or more synthetic steps, are carried out without the separation of any intermediates, so as to reduce time and to save both energy and raw materials.[6, 7] The Hantzsch reaction, which provides 1,4-dihydropyridines as products, is one of the most well-known MCRs. There is always something new on this old topic.[8] This is mainly due to the fact that the 1,4-dihydropyridines exhibit significant pharmacological and biological functions such as calcium channel blocking[9], anti-anginal[10], antitumor[11], anti-inflammatory[12, 13] antitubercular[14], analgesic[15] and antithrombotic activites.[16, 17] Moreover 1,4-dihydropyridine skeleton is the parent nucleus of many commercial drugs such as amlodipine, nifedipin, nimodipin, felodipine, isradipine, and nicardipine. Thus, 1,4-dihydropyridines have attracted the attention of many chemists and pharmacologists. As a result, various methods to prepare these compounds have been reported.[18-24]

More recently, the design of magnetical catalysts has attracted a great deal of attention because these catalysts improve the efficient separation of catalysts by magnetic decantation after the reaction leading to improved reusability.[25-27] The combination of this concept with that of nano materials holds a significant potential in advanced catalysts with improved activities and selectivities providing high specific surface area to volume ratio and higher surface area affording more active sites. Thus making MNPs have emerged as a new class of nano catalysts.[28, 29] MNPs are one of the most extensively considered materials in research fields including biotechnology, biomedicine and catalysis. These are generally inert and, for this reason, ideal for imaging and separation in biological systems.[30, 31] They have been used as a

Department of Organic Chemistry, Faculty of Chemistry, University of Kashan,Kashan, I.R. Iran. E-mail: bamoniri@kashanu.ac.ir
† Footnotes relating to the title and/or authors should appear here. Electronic Supplementary Information (ESI) available: [details of any supplementary information available should be included here]. See DOI: 10.1039/x0xx00000x

useful support in a variety of heterogeneous catalysts for various organic reactions.[32-34] MNPs of Fe_3O_4 are an efficient and important alternative to conventional heterogeneous catalyst supports due to their magnetic properties which facilitate the separation of the catalyst upon reaction and produce a very active surface area for adsorptions or immobilization of metals and ligands.[4, 35] Nano-Fe_3O_4 (Fe_3O_4 NPs) is chemically stable, readily available, and easy to prepare, and low in toxicity and cost. However, pure Fe_3O_4 NPs suffer from some inherent limitations: they are oxidized and easily lose their magnetism when used under acidic conditions and they are easy to agglomerate and lose dispersibility.[36, 37] The above inherent limitations of Fe_3O_4 NPs has led to use of a suitable protective coating. Silica has been considered as one of the most ideal coating layers for Fe_3O_4 NPs due to its chemical stability, biocompatibility, flexibility and reactivity with numerous coupling agents.[38] The iron-oxide with a layer of silica not only stabilizes the nanoparticles in solution but also offers sites for surface modification with various biomedical ligands in biological applications,[39,40] Bi_2WO_6, TiO_2 in photocatalyst application[41,42] and γ-mercapto-propyl-trimethoxy-silane for extracted various ions metal from water in a wide pH range.[43]

To the best of our knowledge, To the best of our knowledge, the grafting of $SnCl_4$ on Fe_3O_4 coated with SiO_2 has not been reported previously.In this study, we report, for the first time, the successful synthesis of Fe_3O_4@SiO_2-$SnCl_4$ as a new catalyst for the synthesis of 1,4-dihydropyridines. We attempted to perform one-pot synthesis of 1,4-dihydropyridine derivatives through three and four component coupling reaction of aldehydes, 1,3-dicabonyl compounds, and ammonium acetate in the presence of Fe_3O_4@SiO_2-$SnCl_4$ as an efficient eco-friendly catalyst under ultrasound irradiation.

Experimental

Materials and apparatus

Chemicals and solvents were purchased from Merck and Aldrich companies. FT-IR spectra were run on a Nicolet Magna 550 spectrometer using KBr pellets. NMR spectra were recorded at 400 MHz (^{1}H) on a Bruker DRX-400 Avance spectrometer in $CDCl_3$ as a solvent. Melting points were obtained with a micro melting point apparatus (Electrothermal, Mk3) and used uncorrected. A multiwave ultrasonic generator (Sonicator 3000; Bandelin MS 72, Germany), equipped with a convertor/transducer and titanium oscillator (horn), 12.5 mm in diameter, operating at 20 kHz with a maximum power output of 60 W, was used for the ultrasonic irradiation. The ultrasonic generator automatically adjusted the power level. The morphology of the synthesized samples and catalyst were studied by a Mira II LMU Tescan FE-SEM made in Czech Republic. XRD patterns were recorded on a Philips Xpert MPD diffractometer equipped with a Cu Kα anode (λ=1.54 A˚) in the 2θ range from 10 to 80˚. Magnetization of the samples was recorded as a function of the applied magnetic field sweeping between ±10 kOe at room temperature. All measurements were performed on a vibrating sample magnetometer device (Meghnatis Daghigh Kavir Co., Kashan Kavir, Iran). Fe_3O_4@SiO_2-$SnCl_4$ average size and distribution were analyzed by TEM using a Philips CM120 with a LaB6 cathode and accelerating voltage of 120 kV. Elemental composition of the above mentioned MNPs was investigated by EDX spectroscopy (XL30, Philips microscope). The specific surface area was evaluated by the BET method using N_2 adsorption at –196 °C using an automated gas adsorption analyzer (TriStar II 3020 V1.03, Micromeritics).

Synthesis of Fe_3O_4@SiO_2-$SnCl_4$ MNPs

Fe_3O_4 nanoparticles were prepared by a known procedure, chemical co-precipitation method reported in the literature.[44, 45] Briefly, $FeCl_3{\cdot}6H_2O$ (2.7 g) and $FeCl_2{\cdot}4H_2O$ (1 g) with molar ratio of 2:1, were dissolved in concentrated HCl, 1.2 M (100 mL, 0.12 mol) through ultrasonic method for 30 min. Then, ammonia 1.25 M (150 mL, 0.19 mol) was injected into the reaction mixture under vigorous stirring at 80 ˚C for 1 h under atmosphere nitrogen. The black magnetic nanoparticles of Fe_3O_4 (magnetite) were formed. Afterwards, the reaction mixture was cooled. The precipitate was isolated using the magnetic field and washed thoroughly with water until the supernatant liquid reached neutrality (pH ~7).

The synthesized Fe_3O_4 MNPs were used for coating with a silica shell following the reported method.[46] Fe_3O_4 MNPs (1 g) were diluted by the consecutive addition of water (20 mL), ethanol (60 mL), and concentrated aqueous ammonia (2 mL, 25 wt%). The resultant dispersion was homogenized through ultrasonic method. A solution of tetraethylorthosilicate (TEOS) (0.5 mL) in ethanol (10 mL) was then added to the dispersion in a drop-wise manner at room temperature under vigorous stirring for 16 h. Fe_3O_4@SiO_2 was collected by an external magnet, washed three times with ethanol (30 mL) and dried under vacuum at 70 ˚C for 6 h.

In the last step, Fe_3O_4@SiO_2 (0.65 g) was dispersed in $CHCl_3$ (10 mL) using ultrasonic method for 30 min. Subsequently, $SnCl_4$ (0.16 mL, 0.001 mol) was added drop-wise to dispersed solution of Fe_3O_4@SiO_2 at room temperature under vigorous stirring over a period of 30 min. The resulting suspension was separated using an external magnet, washed with chloroform (20 mL) and dried at room temperature to obtain the brown solid presented nano Fe_3O_4@SiO_2–$SnCl_4$

Acidic capacity of Fe_3O_4@SiO_2-$SnCl_4$

100 mg of Fe_3O_4@SiO_2-$SnCl_4$ accurately weighted placed in conical flask containing about 10 mL of water and 3 drops of phenolphthalein TS and then titrated with NaOH (0.1 M) VS until solution remained light pink for 30 seconds.

General procedure for the synthesis of 1,4-dihydropyridines

Method I (Δ)

A mixture of an aryl aldehyde (1 mmol), 1,3-dicarbonyl compound (2 mmol), ammonium acetate (1.5 mmol) and Fe_3O_4@SiO_2-$SnCl_4$ (25 mg) was refluxed in ethanol (5 mL) near 75 °C for the stipulated time mentioned in table 3. The progress of the reaction was monitored by TLC (EtOAc: petroleum ether 7: 3). After completion of the reaction, the catalyst was separated by an external magnet and reused for the next experiment. The filtrate was poured into crushed ice obtaining solid product, recrystallized from ethanol to get pure crystalline 1,4-dihydropyridines derivative.

Method II (US)

In a round-bottom flask, a mixture of an aryl aldehyde (1 mmol), 1,3-dicarbonyl compound (2 mmol), ammonium acetate (1.5 mmol) and Fe_3O_4@SiO_2-$SnCl_4$ (18mg) in ethanol (5 mL) was sonicated at 20 kHz frequency and 40W power at room temperature for the stipulated time which was confirmed by TLC and worked-up as described in method I.

Spectral data for selected compounds

2,6-Dimethyl-4-phenyl-1,4-dihydropyridine-3,5-diethylcarboxylate (compound 4a) Yellowish solid, FT-IR (KBr, υ cm^{-1}): 3342 (NH), 1689 (C=O, ester), 1487 (C=C, aromatic), 1212 (C-O). ^{1}H NMR ($CDCl_3$, 400 MH) δ: 7.28 (d, *J*= 7 Hz, 2H. Ar-H), 7.21 (t, *J*= 6.9 Hz, 2H. Ar-H), 7.13 (d, *J*= 6.9 Hz, 1H, Ar-H), 5.54(s, 1H, NH), 4.99 (s, 1H, CH), 4.09(q, *J* = 6.8 Hz, 4H, 2 OCH_2), 2.34 (s, 6H, $2CH_3$), 1.22 (t, *J* = 6.8 Hz, 6H, $2CH_3CH_2$).

2,6-Dimethyl-4-(4-methoxyphenyl)-1,4-dihydropyridine-3,5-diethylcarboxylate (compound 4b) Yellow solid, FT-IR (KBr, υ cm^{-1}): 3343 (NH), 1689 (C=O, ester), 1489 (C=C, aromatic), 1211 (C-O). ^{1}H NMR ($CDCl_3$, 400 MH) δ: 7.20 (d, *J*= 7.9 Hz, 2H. Ar-H), 6.75 (d, *J*= 7.9 Hz, 2H, Ar-H), 5.54(s, 1H, NH), 4.93 (s, 1H, CH), 4.10(q, *J* = 7.4 Hz, 4H, 2 OCH_2), 3.76 (s, 3H, OCH_3), 2.33 (s, 6H, $2CH_3$), 1.23 (t, *J* = 7.4 Hz, 6H, $2CH_3CH_2$).

2,6-Dimethyl-4-(4-chlorophenyl)-1,4-dihydropyridine-3,5-diethylcarboxylate (compound 4c) Yellowish solid, FT-IR (KBr, υ cm^{-1}): 3356 (NH), 1695 (C=O, ester), 1486 (C=C aromatic), 1214 (C-O), 1117 (C-Cl). ^{1}H NMR ($CDCl_3$, 400 MH) δ: 7.22 (d, *J*= 8 Hz, 2H. Ar-H), 7.17 (d, *J*= 8 Hz, 2H, Ar-H), 5.55(s, 1H, NH), 4.96 (s, 1H, CH), 4.08(q, *J* = 7.2 Hz, 4H, 2 OCH_2), 2.34 (s, 6H, $2CH_3$), 1.22 (t, *J* = 7.2 Hz, 6H, $2CH_3CH_2$)

2,6-Dimethyl-4-(4-nitrophenyl)-1,4-dihydropyridine-3,5-diethylcarboxylate (compound 4d) Colorless solid, FT-IR (KBr, υ cm^{-1}): 3327 (N-H), 1696 (C=O, ester), 1517 (NO_2), 1486 (C=C, aromatic), 1345 (NO_2), 1213 (C-O); ^{1}H NMR ($CDCl_3$, 400 MH) δ (ppm): 8.09 (d, J = 7.9 Hz, 2H, Ar-H), 7.45 (d, J= 7.9 Hz, 2H, Ar-H), 5.63 (s, 1H, NH), 5.10 (s, 1H, CH), 4.08 (q, J = 7.4 Hz, 4H, 2 OCH_2), 2.37 (s, 6H, 2 CH_3), 1.24 (t, J = 7.4 Hz, 6H, 2 CH_3CH_2).

3,3,6,6-Tetramethyl-9-4-phenyl-3,4,6,7-tetrahydroacridine 1,8(2H,5H,9H,10H)-dione (compound 4e) Yellowish solid, FT-IR (KBr, υ cm^{-1}): 3279(NH), 1641 (C=O, dimedone), 1484 (C=C, aromatic). ^{1}H NMR ($CDCl_3$, 400 MHz) δ: 7.33 (d, *J* = 7.5 Hz, 2H, Ar-H), 7.19 (t, *J* = 7.5 Hz, 2H, Ar-H), 7.07 (t, *J* = 7.5 Hz, 1H, Ar-H), 6.68 (s, 1H, NH), 5.08 (s, 1H, CH), 2.14–2.39 (m, 8H, 4 CH_2), 1.08 (s, 6H, 2 CH_3), 0.97 (s, 6H, 2 CH_3).

3,3,6,6-Tetramethyl-9-(4-methoxyphenyl)-3,4,6,7-tetrahydroacridine-1,8 (2H,5H,9H,10H) -dione (compound 4f) Yellow solid, FT-IR (KBr, υ cm^{-1}) 3279 (NH), 1640 (C=O, dimedone), 1482 (C=C aromatic), 1224 (C-O); ^{1}H NMR ($CDCl_3$, 400 MHz) δ (ppm): 7.23 (d, J = 8.3 Hz, 2H, Ar-H), 6.72 (d, J = 8.3 Hz, 2H, Ar-H), 6.51 (s, 1H, NH), 5.02 (s, 1H, CH), 3.70 (s, 3H, OCH_3), 2.14- 2.37 (m, 8H, 4 CH_2), 1.08 (s, 6H, 2 CH_3), 0.96 (s, 6H, 2 CH_3).

3,3,6,6-Tetramethyl-9-(4-chlorophenyl)-3,4,6,7-tetrahydroacridine1,8(2H,5H,9H,10H) -dione (compound 4g) Yellow solid, FT-IR (KBr, υ cm^{-1}) 3279 (NH) , 1644 (C=O, dimedone), 1486 (C=C, aromatic), 1145 (C-Cl). ^{1}H NMR ($CDCl_3$, 400 MHz) δ: 7.27 (d, *J* = 8 Hz, 2H, Ar-H), 7.17 (d, *J* = 8 Hz, 2H, Ar-H), 6.79 (s, 1H, NH), 5.05 (s, 1H, CH), 2.13- 2.37 (m, 8H, 4 CH_2), 1.08 (s, 6H, 2 CH_3), 0.96 (s, 6H, 2 CH_3).

3,3,6,6-Tetramethyl-9-(4-nitrophenyl)-3,4,6,7-tetrahydroacridine-1,8(2H,5H,9H,10H)-dione (compound 4h) Yellow-orange solid, FT-IR (KBr, υ cm^{-1}) 3384 (NH), 1643 (C=O, dimedone), 1514 (NO_2), 1481 (C=C, aromatic), 1344 (NO_2). ^{1}H NMR ($CDCl_3$, 400 MHz) δ: 8.07 (d, *J* = 8.3 Hz, 2H, Ar-H), 7.51(d, *J* = 8.3 Hz, 2H, Ar-H), 6.13 (s, 1H, NH), 5.15 (s, 1H, CH), 2.14- 2.45 (m, 8H, 4 CH_2), 1.10 (s, 6H, 2 CH_3), 0.96 (s, 6H, 2 CH_3).

2,7,7-Trimethyl-5-oxo-4-phenyl-1,4,5,6,7,8-hexahydroquinoline-3-carboxylic acid ethyl ester (compound 4i) Yellowish solid, FT-IR (KBr, υ cm^{-1}): 3289 (NH), 1698 (C=O, ester), 1640 (C=O, dimedone), 1485 (C=C, aromatic), 1215 (C-O). ^{1}H NMR ($CDCl_3$, 400 MHz) δ: 7.30 (d, *J* = 7.5 Hz, 2H, Ar-H), 7.19 (t, *J* = 7.5 Hz, 2H, Ar-H), 7.09 (t, *J* = 7.2 Hz, 1H, Ar-H), 6.44 (s, 1H, NH), 5.05 (s, 1H, CH), 4.06 (q, *J* =7.2 Hz, 2H, OCH_2), 2.35 (s, 3H, CH_3), 2.13–2.30 (m, 4H, 2 CH_2), 1.18 (t, *J* =7.2 Hz, 3H, CH_3CH_2), 1.07 (s, 3H, CH_3), 0.93 (s, 3H, CH_3).

2,7,7-Trimethyl-5-oxo-4-(4-methoxyphenyl)-1,4,5,6,7,8-hexahydroquinoline-3-carboxylic acid ethyl ester (compound 4j) Yellow solid, FT-IR (KBr, υ cm^{-1}): 3279 (NH), 1700 (C=O, ester), 1645 (C=O, dimedone), 1497 (C=C, aromatic), 1217 (C-O). ^{1}H NMR ($CDCl_3$, 400 MHz) δ: 7.73 (d, *J* =8 Hz, 2H, Ar-H), 7.10 (d, *J*= 8 Hz, 2H, Ar-H), 5.99 (s, 1H, NH), 4.99 (s, 1H, CH), 4.06 (q, *J*= 6.8 Hz, 2H, OCH_2), 3.73 (s, 3H, OCH_3), 2.36 (s, 3H, CH_3), 2.13–2.34 (m, 4H, 2 CH_2), 1.20 (t, *J*= 6.8 Hz, 3H, CH_3CH_2), 1.07 (s, 3H, CH_3), 0.94 (s, 3H, CH_3).

2,7,7-Trimethyl-5-oxo-4-(4-chlorophenyl)-1,4,5,6,7,8-hexahydroquinoline-3-carboxylic acid ethyl ester (compound 4k) Yellow solid, FT-IR (KBr, υ cm^{-1}): 3276 (NH), 1703 (C=O, ester), 1645 (C=O, dimedone), 1490 (C=C, aromatic), 1217 (C-O), 1158 (C-Cl). ^{1}H NMR ($CDCl_3$, 400 MHz) δ: 7.26 (d, *J* =6.9 Hz, 2H, Ar-H), 7.16 (d, *J*= 6.9 Hz, 2H, Ar-H), 6.00 (s, 1H, NH), 5.02 (s, 1H, CH), 4.06 (q, *J*= 6.8 Hz, 2H, OCH_2), 2.38 (s, 3H, CH_3), 2.13–2.31 (m, 4H, 2 CH_2), 1.19 (t, *J*= 6.8 Hz, 3H, CH_3CH_2), 1.08 (s, 3H, CH_3), 0.93 (s, 3H, CH_3).

2,7,7-Trimethyl-5-oxo-4-(4-nitrophenyl)-1,4,5,6,7,8-hexahydroquinoline-3-carboxylic acid ethyl ester (compound 4l) Yellow solid, FT-IR (KBr, υ cm^{-1}): 3279 (NH), 1702 (C=O, ester), 1647 (C=O, dimedone), 1516 (NO_2), 1344 (NO_2); ^{1}H NMR ($CDCl_3$, 400 MHz) δ (ppm): 8.08 (d, J =7.9 Hz, 2H, Ar-H), 7.48 (d, J= 7.9 Hz, 2H, Ar-H), 5.91 (s, 1H, NH), 5.15 (s, 1H, CH), 4.05 (q, J= 7.1 Hz, 2H, OCH_2), 2.42 (s, 3H), 2.10–2.36 (m, 4H, 2 CH_2), 1.17 (t, J= 7.1 Hz, 3H, CH_3CH_2), 1.09 (s, 3H, CH_3), 0.91 (s, 3H, CH_3).

Results and discussion

This research was performed in two steps. Firstly, Fe_3O_4@SiO_2-$SnCl_4$ MNPs were prepared and identified by FT-IR, XRD, VSM, FE-SEM, EDS, and TEM techniques. In the second step, 1,4-dihydropyridine derivatives were synthesized by aryl

aldehydes, 1,3-dicarbonyl compounds, and ammonium acetate under reflux and ultrasound irradiation methods and then characterized by their melting points using FT-IR, ^{1}HNMR spectroscopy.

Preparation and characterization of Fe_3O_4@SiO_2–$SnCl_4$

Fe_3O_4@SiO_2-$SnCl_4$ was prepared by a simple, low cost and convenient method (Figure1).

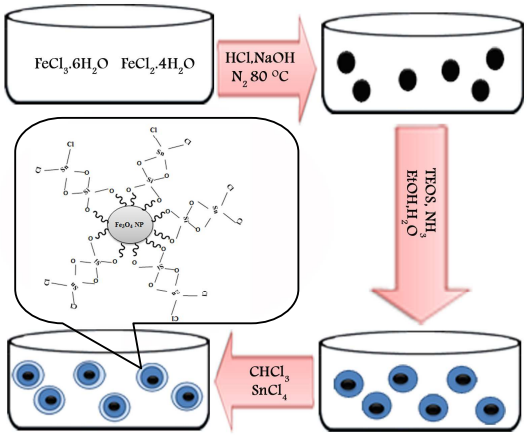

Fig. 1. The schematic diagram for synthesis and suggested structure of Fe_3O_4@SiO_2-$SnCl_4$

In order to recognize the molecular structures of Fe_3O_4, Fe_3O_4@SiO_2, and Fe_3O_4@SiO_2– $SnCl_4$ MNPs, FT-IR analysis of the three mentioned samples was performed (Figure 2). Fe_3O_4 was identified by bands at 443 and 582 cm^{-1} due to Fe–O vibrations in octahedral and tetrahedral sites[47] (Figure 1a). The FT-IR spectrum of Fe_3O_4@SiO_2 (Figure 2b) displays characteristic peaks at 1094 and 802 cm^{-1} corresponding to symmetrical and asymmetrical vibrations of Si–O–Si, respectively. Weak band at 469 cm^{-1} corresponds to the Si–O–Fe stretching vibrations of the Fe_3O_4@SiO_2. These outcomes indicate that SiO_2 is immobilized on the surface of Fe_3O_4. The successful covalent linking of the $SnCl_4$ on the surface of Fe_3O_4@SiO_2 was confirmed by the appearance of a new band at 563 cm^{-1}, which originates from the absorption of O-Sn (Figure 2d).[48,49]

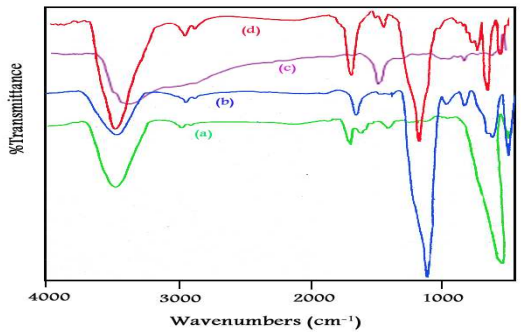

Fig. 2. FT-IR spectra of (a) Fe_3O_4, (b) Fe_3O_4@SiO_2, (c) $SnCl_4$ and (d) Fe_3O_4@SiO_2-$SnCl_4$

The phase and purity of the different stepwise synthesized materials in this work from magnetite Fe_3O_4 to final catalyst Fe_3O_4@SiO_2-$SnCl_4$ were determined by XRD patterns (Figure 3). XRD pattern of Fe_3O_4 exhibited peaks at 2θ=30.43, 35.80, 43.40, 53.98, 57.46, 62.99, and 74.51° (Figure 3a). The diffraction peaks in this pattern can be in accord with standard pattern of an inverse cubic spinel of Fe_3O_4.[50] The strong and sharp peaks indicated phase purity of Fe_3O_4 nanoparticles. Silica coated magnetite nano particles exhibited a broadened pattern due to the non-crystalline nature at 2θ= 20-30 corresponding to amorphous phase of SiO_2 and also 30.33, 35.79, 43.36, 53.82, 57.36, 62.99 and 74.62° which corresponded to Fe_3O_4 structure (Figure 3b).The XRD pattern of Fe_3O_4@SiO_2-$SnCl_4$ in figure 3c showed a much broader diffraction pattern and increased the noise to that of figure 3b, which seems to link to $SnCl_4$ on the surface of Fe_3O_4@SiO_2. Moreover, characteristic peaks of Fe_3O_4 were observed in three samples, indicating that the binding process did not induce any phase change.

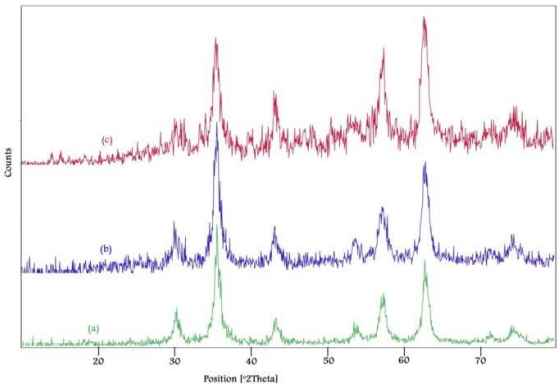

Fig. 3. XRD patterns of (a) Fe_3O_4, (b) Fe_3O_4@SiO_2, and (c) Fe_3O_4@SiO_2-$SnCl_4$

The energy dispersive X-ray (EDX) from the Fe_3O_4@SiO_2-$SnCl_4$ (Figure 4) provided the presence of the expected elements in the structure of this catalyst and confirmed supporting of $SnCl_4$ on Fe_3O_4@SiO_2. The elemental compositions of Fe_3O_4@SiO_2-$SnCl_4$ were found to be 52.80, 31.33, 0.82, 5.30 and 9.76% for Fe, O, Si, Sn and Cl, respectively.

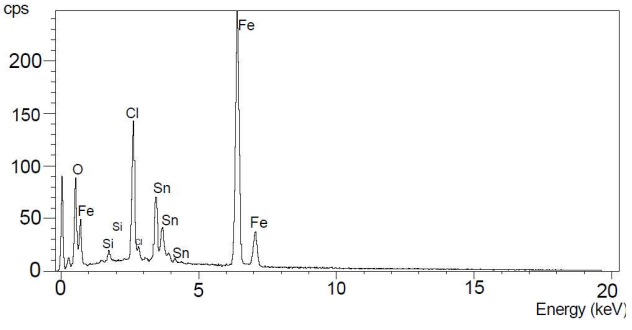

Fig. 4. EDX patterns of Fe_3O_4@SiO_2-$SnCl_4$

The BET specific surface area of Fe_3O_4@SiO_2-$SnCl_4$ in this study was 59.0467 m^2/g. In order to identify the possible structure of Fe_3O_4@SiO_2-$SnCl_4$, we determined acidic capacity of this catalyst by

titration producing HCl in water. We found that 0.1 g of the catalyst produced 0.324 mmol of H^+ or Cl^-. Also, for the determination of the loading amounts of the Sn on the Fe_3O_4@SiO_2-$SnCl_4$ by the addition of 1 mL aqueous solution of NaOH (0.2 M) to 0.1 g of catalyst and hot water. The nanomagnetic catalyst was separated with external magnet from the obtained $Sn(OH)_4$ solution. The solution was evaporated to obtain a dry $Sn(OH)_4$ powder. The calculated loading amount of Sn in the catalyst was 0.138 mmol g^{-1}. According to the above data and EDX data, the molar ratio of Sn:Cl, were investigated 1:2 and the possible structure of Fe_3O_4@SiO_2-$SnCl_4$ was proposed as shown in figure 5.

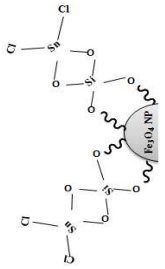

Fig. 5. Suggested structure of Fe_3O_4@SiO_2-$SnCl_4$

The magnetization curve for synthesized Fe_3O_4, Fe_3O_4@SiO_2, and Fe_3O_4@SiO_2–$SnCl_4$ nanoparticles is shown in figure 6. Room temperature specific magnetization (M) versus applied magnetic field (H) indicated the magnetization as a function of applied magnetic field. The saturation magnetization of the Fe_3O_4 nanoparticles was about 53.52 emu/g, which decreased to 40.98 emu/g after supporting Fe_3O_4 with SiO_2 and to 31.05 emu/g after supporting Fe_3O_4@$SiO_2$with $SnCl_4$. The decrease of the saturation magnetization after surface coating of Fe_3O_4 confirms the presence of a diamagnetic outer shell (SiO_2 or SiO_2-$SnCl_4$).

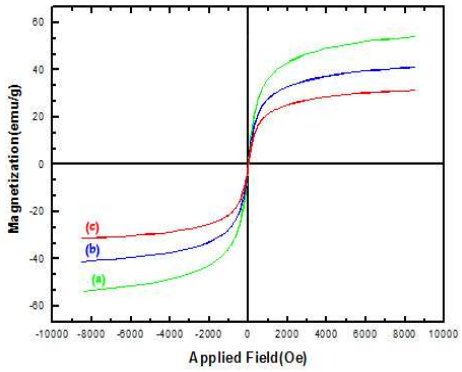

Fig. 6. VSM patterns of (a) Fe_3O_4, (b) Fe_3O_4@SiO_2, and (c) Fe_3O_4@SiO_2-$SnCl_4$

The FE-SEM images of the Fe_3O_4, Fe_3O_4@SiO_2, and Fe_3O_4@SiO_2–$SnCl_4$ nanoparticles are displayed in figure 7. These images evidently show the surface morphology of three kinds of synthesized MNPs with a nearly spherical shape. Although Fe_3O_4@SiO_2 and Fe_3O_4@SiO_2-$SnCl_4$ still keep the morphological of Fe_3O_4, they are slightly larger in particle size.

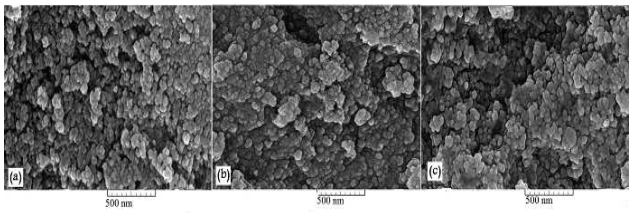

Fig. 7. SEM images of (a) Fe_3O_4, (b) Fe_3O_4@SiO_2, and (c) Fe_3O_4@SiO_2-$SnCl_4$

Transmission electron microscopy (TEM) image of the synthesized catalyst was recorded as depicted in figure 8. According to this image, the catalyst was approximately 28 nm in size.

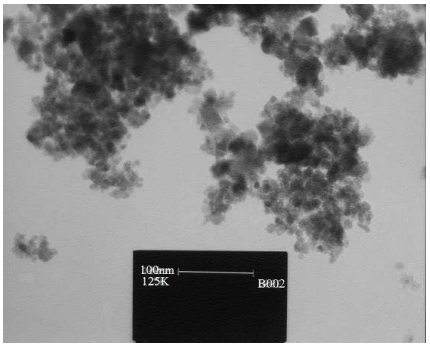

Fig. 8. TEM image of Fe_3O_4@SiO_2-$SnCl_4$

Evaluation of the catalytic activity of Fe_3O_4@SiO_2–$SnCl_4$

To obtain appropriate conditions for the synthesis of 1,4-dihydropyridines, different reaction conditions have been examined. At the outset, the reaction was carried out with benzaldehyde, ethyl acetoacetate, dimedone and ammonium acetate as a model reaction (Scheme 1).

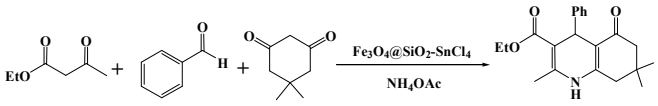

Scheme 1. Standard model reaction

We studied the effect of various solvents such as H_2O, EtOH, DMF, CH_3CN, and $CHCl_3$ on a model reaction under ultrasound irradiation (40W power). The results are summarized in table 1. It was found that ethanol was the best choice for the model reaction.

Table 1 Optimization of the model reaction using various solvents under ultrasound irradiation

Entry	Solvent	Time (min)	Yield (%)[a]
1	CH_3CN	5	74
2	$CHCl_3$	5	75
3	DMF	5	85
4	Water	5	89
5	EtOH	5	98

[a]Isolated yields. benzaldehyde (1 mmol), ethyl acetoacetate (1 mmol), dimedone (1 mmol), ammonium acetate (1.5 mmol) and Fe_3O_4@SiO_2-$SnCl_4$ (18mg).

In order to study the effects of $Fe_3O_4@SiO_2$-$SnCl_4$ on the model reaction, catalytic behaviour of $Fe_3O_4@SiO_2$-$SnCl_4$ was compared under reflux or and ultrasound irradiation conditions (Table 2). The obtained results showed that, in the absence of catalyst, no significant product was obtained and in the presence of $Fe_3O_4@SiO_2$-$SnCl_4$ the reaction was carried out with high yields (Entry 1). Also the results in table 1 exhibit the optimum amount of the catalyst was 25 mg under reflux condition, and 18 mg under ultrasound irradiation (Entry 6). Notably, the increase of the catalyst in reflux and ultrasound irradiation conditions did not show any significant changes in yield and time of reaction (Entry 7).

Table 2 Optimization of the model reaction using $Fe_3O_4@SiO_2$-$SnCl_4$ under reflux (I) and ultrasound irradiation (II)

Entry	Method I (Δ)		Method II (US)	
	Catalyst/ (g)		Catalyst/ (g)	
	Time (min)	Yield (%)[a]	Time (min)	Yield (%)[a]
1	none		none	
	200	trace	20	trace
2	$SnCl_4$ / 0.13		$SnCl_4$ / 0.13	
	30	49	10	56
3	$BF_3{\cdot}Et_2O$ / 0.13		$BF_3{\cdot}Et_2O$ / 0.13	
	30	50	10	55
4	$TiCl_4$ / 0.13		$TiCl_4$ / 0.13	
	30	45	10	50
5	$SnCl_4{\cdot}SiO_2$ / 0.50		$SnCl_4{\cdot}SiO_2$ / 0.50	
	30	55	10	78
6	$Fe_3O_4@SiO_2$-$SnCl_4$/ 0.005		$Fe_3O_4@SiO_2$-$SnCl_4$/ 0.005	
	25	65	8	84
7	$Fe_3O_4@SiO_2$-$SnCl_4$/ 0.010		$Fe_3O_4@SiO_2$-$SnCl_4$/ 0.010	
	23	73	6	89
8	$Fe_3O_4@SiO_2$-$SnCl_4$/ 0.020		$Fe_3O_4@SiO_2$-$SnCl_4$/ 0.015	
	18	85	5	91
9	$Fe_3O_4@SiO_2$-$SnCl_4$/ 0.025		$Fe_3O_4@SiO_2$-$SnCl_4$/ 0.018	
	14	95	5	98
10	$Fe_3O_4@SiO_2$-$SnCl_4$/ 0.030		$Fe_3O_4@SiO_2$-$SnCl_4$/ 0.025	
	14	94	5	96

[a]Isolated yields. benzaldehyde (1 mmol), ethyl acetoacetate (1 mmol), dimedone (1 mmol) and ammonium acetate (1.5 mmol) in ethanol (5 mL)

In order to examine the scope and generality of this procedure in these methodologies, a number of aromatic aldehydes containing both electron-withdrawing and electron-donating groups in the para position were used with ammonium acetate and ethyl acetoacetate or/and dimedone in the presence of $Fe_3O_4@SiO_2$-$SnCl_4$ in ethanol under reflux and ultrasound irradiation conditions. By comparing obtained data for different condition from Table 3, reveal that ultrasound irradiation method leads to interesting effect concerning the synthesis of 1,4-dihydropyridines.

In all cases, when the reactions were carried out under ultrasound irradiation, the times of the reactions were shorter and the yields of the products were higher than reflux method. Also, the amount of catalyst was decreased under ultrasound irradiation. This should be explained based on the phenomenon of cavitation produced by ultrasound irradiation. Moreover this method, particularly when considering the basic green chemistry concepts, is more environmental friendly. As can be seen from the results in Table 3, aromatic aldehydes with substituents carrying either electron-donating or electron-withdrawing groups reacted successfully with 1,3-dicabonyl compounds to afford the corresponding 1,4-dihydropyridines in excellent yields. However, using dimedone instead of ethyl acetoacetate affects the yield and reaction time due to acidity of the methylenic protons.

The proposed mechanism for the formation of 1,4-dihydropyridines in the presence of $Fe_3O_4@SiO_2$-$SnCl_4$, which can act as Lewis acid catalyst (empty π orbital of Sn in $Fe_3O_4@SiO_2$-$SnCl_4$) is depicted in scheme 2.

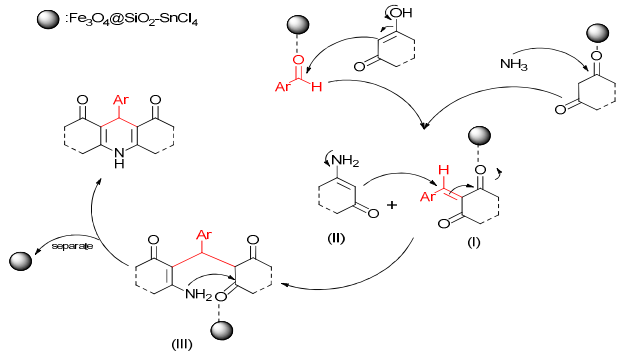

Scheme 2. Proposed mechanism for the synthesis of 1,4-dihydropyridines

As can be seen, an acid–base interaction between $Fe_3O_4@SiO_2$-$SnCl_4$ and oxygen in carbonyl bond forms corresponding Knoevenagel product (I) and enamine (II). In the following, Michael addition is occurred between enamine and Knovenagel product for the formation of an open chain intermediate (III). The dipolar transition state is undergone cyclodehydration to furnish the desired product. Moreover, reaction in heterogeneous systems which proceeds *via* ionic intermediate is influenced predominantly through the mechanical effects of cavitation

Table 3 Synthesis of 1,4-dihydropyridine derivatives under reflux conditions and sonication (methods I and II)

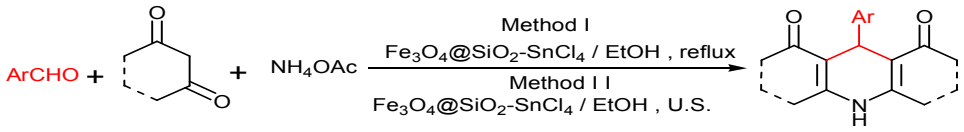

Entry	R	1,3-dicarbonyls		Time(min) / Yield (%)[a]		M. P. (°C)	
		Product		Method I (Δ)[b]	Method II (US)[c]	Found	Reported
1	C_6H_5	Ethyl acetoacetate	Ethyl acetoacetate	25 / 91	6 / 96	157-160	158-160[51]
		4a					
2	4-$MeOC_6H_4$	Ethyl acetoacetate	Ethyl acetoacetate	18 / 89	6 / 92	160-162	161-163[51]
		4b					
3	4-ClC_6H_4	Ethyl acetoacetate	Ethyl acetoacetate	23 / 95	5 / 96	145-147	147-148[51]
		4c					
4	4-$NO_2C_6H_4$	Ethyl acetoacetate	Ethyl acetoacetate	20 / 92	4 / 97	130-132	129-131[51]
		4d					
5	C_6H_5	Dimedone	Dimedone	22 / 93	4 / 96	189-191	190-192[52]
		4e					
6	4-$MeOC_6H_4$	Dimedone	Dimedone	12 / 94	4 / 93	269-271	270-272[52]
		4f					
7	4-ClC_6H_4	Dimedone	Dimedone	15 / 93	3 / 97	297-299	299-230[53]
		4g					
8	4-$NO_2C_6H_4$	Dimedone	Dimedone	15 / 95	3 / 98	285-287	286-288[53]
		4h					
9	C_6H_5	Ethyl acetoacetate	Dimedone	14 / 95	5 / 98	225-227	228-229[54]
		4i					
10	4-$MeOC_6H_4$	Ethyl acetoacetate	Dimedone	15 / 90	5 / 94	258-260	260-262[54]
		4i					
11	4-ClC_6H_4	Ethyl acetoacetate	Dimedone	18 / 96	4 / 96	245-246	245-246[54]
		4k					
12	4-$NO_2C_6H_4$	Ethyl acetoacetate	Dimedone	18 / 95	3 / 98	240-242	241-242[54]
		4l					

[a]Isolated yields. arylaldehyde (1 mmol), 1,3-dicarbonyl compounds (2 mmol), ammonium acetate (1.5 mmol) in ethanol (5 mL)
[b] Fe_3O_4@SiO_2-$SnCl_4$(25mg).
[c]Fe_3O_4@SiO_2-$SnCl_4$(18mg).

Consequently, it is essential for the solid acid to maintain strong acidity even after recycling and the most important benefits for commercial applications. Thus, after the completion of the reaction, the catalyst was separated by an external magnet. The recovered catalyst was washed with chloroform (30 mL) and dried at room temperature without further purification to use for the next run in current reaction under identical condition. It was found that the catalyst could be reused for five times without any appreciable loss of its activity (Figure9).

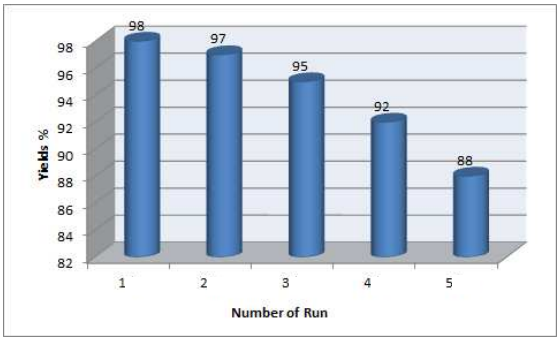

Fig.9. Reusability study of Fe_3O_4@SiO_2-$SnCl_4$

The XRD of the recovered magnetic nanocatalyst was shown in figure 10 and so there is no considerable change in its magnetic phase. The leaching of the catalyst also be examined. Any leaching of catalyst was not observed in this protocol. Therefore, the nanocatalyst is stable during synthesis of 1,4-dihydropyridine under ultrasound irradiation.

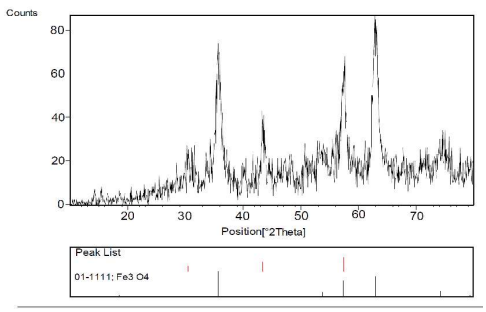

Fig.10. XRD patterns of recovered Fe_3O_4@SiO_2–$SnCl_4$ after five recovery

Conclusions

In conclusion, a convenient and efficient method for the synthesis of 1,4-dihydropyridine derivatives in the presence of Fe_3O_4@SiO_2–$SnCl_4$ as a novel heterogeneous solid acid catalyst has been developed through ultrasound irradiation. This reaction under ultrasound irradiation not only gave excellent yield of products with lesser reaction time but it also required mild reaction conditions and exhibited operational simplicity. In addition, low cost, availability, recyclability and low toxicity of the catalyst make this methodology a valid contribution to the existing processes in the field of one-pot multicomponent Hantzsch reaction.

Acknowledgements

The authors are grateful to University of Kashan for supporting this work by Grant No. (159189/34)

Notes and references

1. F. Bigi, L. Chesini, R. Maggi and G. Sartori, *J. Org. Chem.*, 1999, **64**, 1033-1035.
2. G. Cravotto and P. Cintas, *Chem. Soc. Rev.* , 2006, **35**, 180-196.
3. S. H. Banitaba, J. Safari and S. D. Khalili, *Ultrason. Sonochem.* , 2013, **20**, 401-407.
4. J. Safari and L. Javadian, *Ultrason. Sonochem.* , 2015, **22**, 341-348.
5. N. Moshtael Arani and J. Safari, *Ultrason. Sonochem.* , 2011, **18**, 640-643.
6. M. V. Marques, M. M. Ruthner, L. A. Fontoura and D. Russowsky, *J. Braz. Chem. Soc.* , 2012, **23**, 171-179.
7. I. Devi and P. J. Bhuyan, *Tetrahedron Lett.* , 2004, **45**, 8625-8627.
8. A. Hantzsch, *Justus Liebigs Annalen der Chemie*, 1882, **215**, 1-82.
9. T. Godfraind, R. Miller and M. Wibo, *Pharmacol. Rev.*, 1986, **38**, 321-416.
10. J. G. Breitenbucher and G. Figliozzi, *Tetrahedron Lett.*, 2000, **41**, 4311-4315.
11. R. Boer and V. Gekeler, *Drug. Future*, 1995, **20**, 499-510.
12. V. Briukhanov, I. Zverev and V. Elkin, *Eksperimental'naia i klinicheskaia farmakologiia*, 1994, **57**, 47.
13. S. Bahekar and D. Shinde, *Acta Pharm.*, 2002, **52**, 281-287.
14. G. A. Wächter, M. C. Davis, A. R. Martin and S. G. Franzblau, *J. Med. Chem.*, 1998, **41**, 2436-2438.
15. S. Gullapalli and P. Ramarao, *Neuropharmacol.*, 2002, **42**, 467-475.
16. C. E. Sunkel, M. Fau de Casa-Juana, L. Santos, M. Mar Gomez, M. Villarroya, M. A. Gonzalez-Morales, J. G. Priego and M. P. Ortega, *J. Med. Chem.*, 1990, **33**, 3205-3210.
17. M. O. Handkinura, *Drug Res.*, 1981, **3**, 1131-1134.
18. R. Sridhar and P. T. Perumal, *Tetrahedron*, 2005, **61**, 2465-2470.
19. C. S. Reddy and M. Raghu, *Chin. Chem. Lett.*, 2008, **19**, 775-779.
20. A. Kumar and R. A. Maurya, *Synlett*, 2008, 883-885.
21. M. Hong, C. Cai and W.-B. Yi, *J. Fluorine Chem.*, 2010, **131**, 111-114.
22. M. M. Heravi, K. Bakhtiari, N. M. Javadi, F. F. Bamoharram, M. Saeedi and H. A. Oskooie, *J. Mol. Catal. A, Chem.*, 2007, **264**, 50-52.
23. A. Debache, R. Boulcina, A. Belfaitah, S. Rhouati and B. Carboni, *Synlett*, 2008, 509-512.
24. S. Chandrasekhar, Y. Srinivasa Rao, L. Sreelakshmi, B. Mahipal and C. Raji Reddy, *Synthesis*, 2008, 1737-1740.
25. D. Speliotis, *J. Magn. Magn. Mater.*, 1999, **193**, 29-35.
26. B. Zhen, Q. Jiao, Y. Zhang, Q. Wu and H. Li, *Appl. Catal. A:* 2012, **445**, 239-245.

27. D. m. Lai, L. Deng, J. Li, B. Liao, Q. x. Guo and Y. Fu, *Chem. Sus. Chem*, 2011, **4**, 55-58.
28. T. Hyeon, *Chem. Commun.*, 2003, 927-934.
29. A. H. Lu, W. Schmidt, N. Matoussevitch, H. Bönnemann, B. Spliethoff, B. Tesche, E. Bill, W. Kiefer and F. Schüth, *Angew. Chem.*, 2004, **116**, 4403-4406.
30. L. H. Reddy, J. L. Arias, J. Nicolas and P. Couvreur, *Chem. Rev.*, 2012, **112**, 5818-5878.
31. L. Yan, S. Zhang, P. Chen, H. Liu, H. Yin and H. Li, *Microbiol. Res.*, 2012, **167**, 507-519.
32. K. K. Senapati, S. Roy, C. Borgohain and P. Phukan, *J. Mol. Catal. A: Chem.*, 2012, **352**, 128-134.
33. A. Kotarba, W. Bieniasz, P. Kuśtrowski, K. Stadnicka and Z. Sojka, *Appl. Catal. A:*, 2011, **407**, 100-105.
34. R. N. Baig and R. S. Varma, *Chem. Commun.*, 2012, **48**, 2582-2584.
35. A. H. Latham and M. E. Williams, *Acc. Chem. Res.*, 2008, **41**, 411-420.
36. X. Zhao, Y. Shi, Y. Cai and S. Mou, *Environ. Sci. Technol.*, 2008, **42**, 1201-1206.
37. A. del Campo, T. Sen, J.-P. Lellouche and I. J. Bruce, *J. Magn. Magn. Mater.*, 2005, **293**, 33-40.
38. H.-H. Yang, S.-Q. Zhang, X.-L. Chen, Z.-X. Zhuang, J.-G. Xu and X.-R. Wang, *Anal. Chem.*, 2004, 76, 1316-1321.
39. A. Schätz, M. Hager and O. Reiser, *Adv. Func. Mater.*, 2009, **19**, 2109-2115.
40. S. Ramaprabhu, *Talanta*, 2010, **80**, 2016-2022.
41. S.-H. Chen, Z. Yin, S.-L. Luo, C.-T. Au and X.-J. Li, *Mater. Res. Bull.*, 2013, **48**, 725-729.
42. H. Liu, Z. Jia, S. Ji, Y. Zheng, M. Li and H. Yang, *Catal. Today*, 2011, **175**, 293-298.
43. C. Huang and B. Hu, *Spectrochim. Acta A. Spectro.*, 2008, **63**, 437-444.
44. J. Safari and L. Javadian, *C. R. Chim.*, 2013, **16**, 1165-1171.
45. H. Naeimi and Z. S. Nazifi, *J. Nanopart. Res.* 2013, **15**, 1-11.
46. D. Yang, J. Hu and S. Fu, *J. Phys. Chem. C*, 2009, **113**, 7646-7651.
47. F. Zamani and S. M. Hosseini, *Catal. Commun.*, 2014, **43**, 164-168.
48. K. Niknam, M. A. Zolfigol, D. Saberi and H. Molaee, *J. Chin.Chem. Soc.*, 2009, **56**, 1257-1264.
49. M. Dadkhah and M. Salavati-Niasari, *Mater. Sci. Semicond. Process.*, 2014, **20**, 41-48.
50. A. Bamoniri and N. Moshtael-Arani, *RSC Adv.*, 2015, **5**, 16911-16920.
51. J. J. Vanden Eynde, F. Delfosse, A. Mayence and Y. Van Haverbeke, *Tetrahedron*, 1995, **51**, 6511-6516.
52. M. Q. Nazario Martín, Carlos Seoane, José L. Soto, Arturo Mora, Margarita Suárez, Estael Ochoa, Alhmed Morales and Jose R. Del Bosque *J. Heterocycl. Chem.*, 1995, **32**, 235–238.
53. S. Balalaie, F. Chadegani, F. Darviche and H. R. Bijanzadeh, *Chin. J. Chem.*, 2009, **27**, 1953-1956.
54. B. Bandgar, P. More, V. Kamble and J. Totre, *Arkivoc*, 2008, 1-8.

$SnCl_4$-functionalized nano-Fe_3O_4 encapsulated-silica particles as a novel heterogeneous solid acid for synthesis of 1,4-dihydropyridine derivatives

Abdolhamid Bamoniri*, Sara Fouladgar

Department of Organic Chemistry, Faculty of Chemistry, University of Kashan, Kashan, 8731751167, Iran

E-mail: bamoniri@kashanu.ac.ir

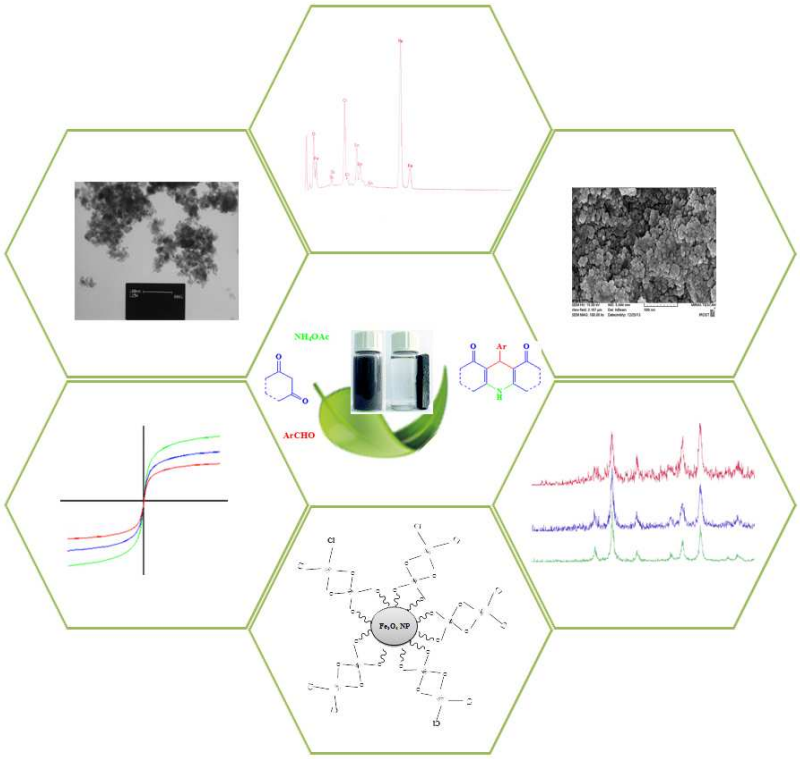

A simple and general synthetic method for the synthesis of 1,4-dihydropyridines *via* three- or four-component condensation of aldehydes, 1,3-dicarbonyl compounds, and ammonium acetate under ultrasonic irradiation were developed by using Fe_3O_4@SiO_2-$SnCl_4$ as an efficient catalyst.